

ACCOUNTS of CHEMICAL RESEARCH[®]

APRIL 2001

Registered in U.S. Patent and Trademark Office; Copyright 2001 by the American Chemical Society

Some Interesting Properties of Metals Confined in Time and Nanometer Space of Different Shapes

MOSTAFA A. EL-SAYED*

Laser Dynamics Laboratory, School of Chemistry and Biochemistry, Georgia Institute of Technology, Atlanta, Georgia 30332-0400

Received April 17, 2000

ABSTRACT

The properties of a material depend on the type of motion its electrons can execute, which depends on the space available for them (i.e., on the degree of their spatial confinement). Thus, the properties of each material are characterized by a specific length scale, usually on the nanometer dimension. If the physical size of the material is reduced below this length scale, its properties change and become sensitive to its size and shape. In this Account we describe some of the observed new chemical, optical, and thermal properties of metallic nanocrystals when their size is confined to the nanometer length scale and their dynamical processes are observed on the femto- to picosecond time scale.

1. Introduction

The physical and chemical properties of a material are determined by the type of motion its electrons are allowed

Mostafa El-Sayed received his B.Sc. from Ain Sham University, Cairo, Egypt, and Ph.D. in 1959 from Florida State University (under M. Kasha). He was a Research Associate at Harvard University, Yale University, and California Institute of Technology before joining the University of California at Los Angeles. In 1994, he became the Julius Brown Chair and the director of the Laser Dynamics Laboratory at Georgia Institute of Technology, where he is now a Regents Professor. He is an elected member of the U.S. National Academy of Sciences and the Third World Academy of Sciences, and a Fellow of the American Academy of Sciences, the AAAS, and the American Physical Society. El-Sayed and his group have numerous publications. Using different laser spectroscopic techniques, they pursued research aimed at elucidating the molecular mechanisms involved in dynamical processes and energy conversion in molecules, in gaseous clusters, and in organic and inorganic solids as well as in photobiological systems. More recently, his group began active research on the ultrafast electron and hole dynamics in semiconductor nanoparticles and the thermal, photothermal and catalytic properties of metallic nanoparticles of different shapes.

to execute. The latter is determined by the space in which the electrons are confined due to the forces they encounter. Unbound (unconfined) electrons have motion that is not quantized and can thus absorb any amount of energy. Once an electron is bound in an atom or in a molecule, its motion becomes highly confined and quantization sets in. The allowed types of motion in atomic or molecular orbitals are found to have well-defined energies. The smaller the space in which the motion is bound, the stronger the confinement and the larger the energy separation between the allowed energies of the different types of motion. The atomic confinement is the strongest type of electronic confined motion. In the hydrogen atom, the electron is confined to a length scale of ~ 50 pm.

In semiconductors, excitation involves the separation of electrons and holes (the charge carriers) by distances that encompass a number of the molecules or ions making up the lattice. Such a distance, known as the Bohr radius, is on the nanometer length scale. The minimum energy required to separate the charge carriers is known as the band gap energy of the semiconductor. What would happen if we were to reduce the physical size of the semiconductor material so it becomes comparable to, or smaller than, the Bohr radius? This would decrease the space in which the charge carriers move, and thus additional quantum confinement would be imposed on their motion. This leads to an increase in the band gap energy, the electron and hole kinetic energy, and the density of the charge carriers within and at the nanoparticle surface. Because of this, as well as the fact that the surface-to-volume ratio greatly increases, new properties not possessed either by the macroscopic semiconductor material or by the individual entity that makes the semiconductor are observed.¹⁻¹³

In a metal, electrons are highly delocalized over large space (i.e., least confined). This is a result of the fact that the separation between the valence and conduction bands vanishes, giving the metal its conducting properties. As we decrease the size of the metal and confine its electronic motion, the separation between the valence and the

* Phone: 404-894-0292. Fax: 404-894-0294. E-mail: mostafa.el-sayed@chemistry.gatech.edu.

TEM Images of Pt Nanoparticles

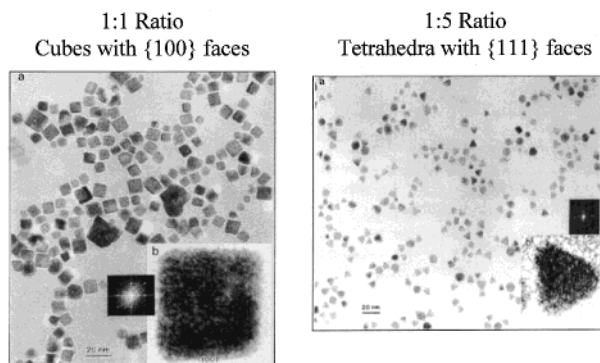


FIGURE 1. Platinum nanoparticles synthesized in colloidal solution and having different shapes (11-nm cubes on the left and ~7-nm tetrahedrons on the right).²⁷ The potential use of these nanoparticles for different types of catalyses drives our research interest in these particles. Do these different shapes have different catalytic properties?

conduction bands becomes comparable to or larger than kT , and the metal becomes a semiconductor. More confinement increases the energy separation further, and the material becomes an insulator. In the size domain at which the metal-to-insulator transition occurs, new properties are expected to be observed which are possessed neither by the metal nor by the molecules or atoms forming the metal.

In noble metals, the decrease in size below the electron mean free path (the distance the electron travels between scattering collisions with the lattice centers) gives rise to intense absorption in the visible–near-UV. This results^{14–17} from the coherent oscillation of the free electrons from one surface of the particle to the other and is called the surface plasmon absorption. Such strong absorption induces strong coupling of the nanoparticles to the electromagnetic radiation of light. This gives these metallic nanoparticles brilliant color in colloidal solution that intrigued scientists in the 17th century. Their technological application was ahead of semiconductor nanoparticles, as they were used to give stained glass its brilliant ruby color used in cathedrals at that time.¹⁸ It was Faraday who showed that the intense color is due to metallic gold in colloidal form. It was not until 1908 when Mie¹⁹ explained the phenomena by solving Maxwell’s equations for the absorption and scattering of electromagnetic radiation by spherical metallic particles. This theory has been used to calculate the spectra of particles smaller than the wavelength of light for nanoparticles whose metallic dielectric function is known and which are embedded in an environment of known dielectric constant.^{15,17,20,21} Colloidal metallic nanoparticles are of interest because of their use as catalysts,²² photocatalysts,²³ sensors,²⁴ and ferrofluids²⁵ and because of their applications in optoelectronics²⁶ and in electronic²⁶ and magnetic²⁴ devices.

Platinum has been synthesized by our group in the 6–10 nm size range *with different shapes*,²⁷ e.g., cubic, tetrahedral, and truncated octahedral. The potential use of metallic nanoparticles of the same metal but with

different shapes in the catalysis of different types of reactions has been suggested.²⁷

While our group is involved in studying the new properties of both semiconductor and metallic nanocrystals, due to space limitations, we limit our discussion in this Account to some of the interesting results our group has observed on two types of metals. These are the thermal and catalytic properties of the transition metals, e.g., platinum and palladium, and the optical and photo-thermal properties of precious metals such as gold.

II. Some Interesting Properties of Metals Confined to the Nanometer Length Scale

A. Transition Metal Nanocrystals of Different Shapes. Transition metal surfaces are known to have very efficient catalytic properties for many important reactions. Since nanoparticles have a good fraction of their atoms present on the surface, their potential use in catalysis is obvious.

Atoms on different types of faces of a single metallic crystal have different electronic structures and thus are expected to have different catalytic properties. In fact, researchers in the high-vacuum surface science and electrochemistry fields have observed different catalytic efficiencies for the different metallic surfaces. We have been able to synthesize platinum nanoparticles having different shapes, and thus having different types of facets. In a *Science* report, we published²⁷ the results of the reduction of $(PtCl_4)^{2-}$ in solution with $H_2(g)$ in the presence of polyacrylate as a capping agent of different concentrations. Figure 1 shows the TEM images of the dominantly 11-nm cubic nanoparticle (left) and the dominantly 7-nm tetrahedral nanoparticle (right). The high-resolution images of each particle, in which the individual atoms are resolved, are shown in (b) of each figure. Other particle shapes have been made (truncated octahedral and polyhedral nanoparticles). While some mechanisms have been proposed for the growth process of these particles,^{28,29} the exact mechanism of the initial nucleation, growth, and shape control is not known. The quality of both the salt and of the polymer as well as that of the water used all seem to affect the outcome of the particle shape distribution. Acrylic acid was also used as a capping material. Cubic particles can be prepared by simply adjusting the pH without the addition of any capping agents. In this case, surface charges could stabilize the individual particles and prevent their aggregation and precipitation. However, these particles are not as stable as those capped with the polymer.

B. Homogeneous Nanocatalysis in Solution. The term “homogeneous catalysis” is used here since solutions of nanoparticles in colloidal preparations are clear, with no observed light scattering. This is due to the fact that these particles are over an order of magnitude smaller than visible light. In this section, the catalysis by the surfaces of the particles, a topic usually discussed under the title of “heterocatalysis”, is discussed.

Size dependence of catalysis of metal clusters is a topic of active research. We have used transition metal nano-

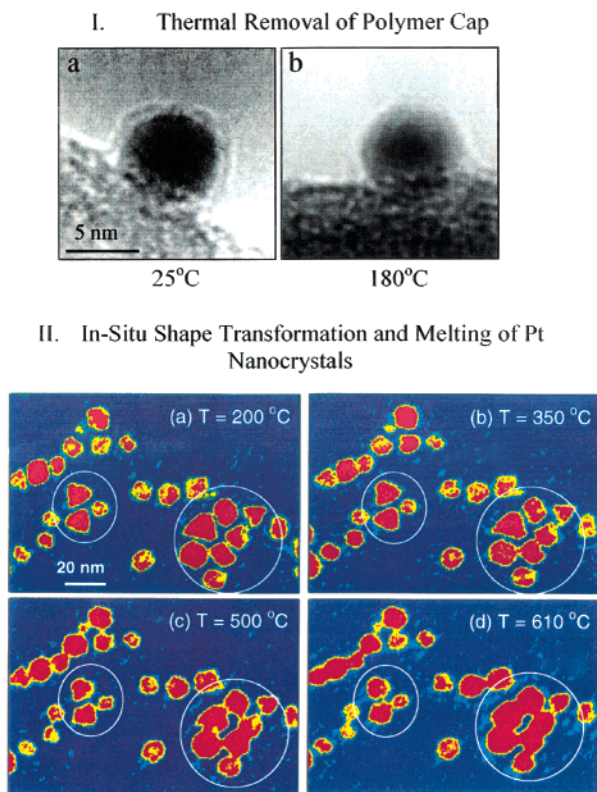
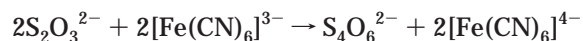


FIGURE 2. Thermal properties of the capped platinum nanoparticles as studied by in situ variable-temperature TEM spectroscopy.³⁵ The capping polymer dissociates at ~ 180 °C (I), and the particle shape is retained up to 400 °C (II). This suggests that after the activation of the nanoparticles by heating them to ~ 200 °C, these solid particles can be used for shape-controlled heterogeneous catalysis from below room temperature up to ~ 400 °C.

particles for the catalysis of two different types of reactions. The first is the electron-transfer reaction:



catalyzed by platinum nanoparticles. The activation energy of this reaction in solution is found to be 38.3 ± 2.0 kJ/mol. When this reaction is carried out in the presence of platinum nanoparticles (with dominant truncated octahedral shapes), the activation energy is found to be reduced³⁰ to 17.6 ± 0.9 kJ/mol. This reaction was previously found to occur on the surface of the nanoparticles by studying the dependence of the catalysis rate on the concentration of the nanoparticle catalyst.³¹

The coupling reaction of arylboronic acid and its derivatives with aryl halides (the Suzuki reaction) in the presence of $\text{Pd}(\text{PPh}_3)_4$ and base to give biaryls was first reported³² in 1981. These reactions are carried out in organic solvents and are catalyzed by various Pd/ligand systems. Phosphine-based palladium catalysts are generally used. One serious problem in homogeneous metal catalysis is the separation of the reaction products from the catalyst. It has been shown that palladium colloids on the nanometer length scale are effective catalysts for the Suzuki reaction³³ in organic solvents. The use of water, however, as a reaction medium for transition-metal-

catalyzed reactions is very attractive for organic synthesis, due to environmental, economic, and safety reasons.

We have found³⁴ that palladium nanoparticles stabilized by poly(*N*-vinyl-2-pyrrolidone) (PVP) are efficient catalysts for the Suzuki reactions between arylboronic acid and aryl halide in aqueous medium. The time dependence of the fluorescence intensity of the biphenyl product in the reaction between iodobenzene and phenylboronic acid is used to determine the initial rate of the reaction as a function of the catalyst concentration. The initial rate is found to depend linearly on the concentration of the Pd catalyst, suggesting that the catalytic reaction occurs on the surface of the Pd nanoparticles.

C. Thermal Properties of Capped Platinum Nanoparticles.³⁵ If platinum nanoparticles of different shapes were to be useful in surface catalysis of gases, such as those used in the petroleum industry or for environmental atmospheric purposes, one would first need to remove the capping material and to make sure that the shape of the dried nanoparticles is thermally stable if the catalytic reaction is to be carried out at high temperatures. Furthermore, if different shapes have different catalytic properties, one needs to know the temperature range in which the shape is preserved.

Figure 2.I shows the temperature effect on the capping polymer as monitored by a variable-temperature TEM system.³⁵ At ~ 180 °C, the capping polymer seems to have thermally desorbed. In the bottom part of the figure (Figure 2.II), the shape stability of the tetrahedral nanoparticle is examined with TEM. The triangular shape seems to be preserved up to 350 °C. At 500 °C, the particles begin to change their shape to spherical, which has the lowest surface energy and thus is the most stable form of the nanoparticle. At 600 °C, surface melting becomes clear, which leads to particle surface amalgamation. Electron diffraction studies³⁵ showed that $\sim 25\%$ of the particle has surface melted at this temperature, leaving the interior crystalline. From these studies, one concludes that, in order to use these particles in heterogeneous catalysis, they should first be heated (activated) to ~ 200 °C to remove the capping polymer. These “activated” nanoparticles can now be useful for shape-controlled catalysis in a temperature range from below room temperature to ~ 750 K. Shape deformation begins to set in, and shape-controlled catalysis would then be lost above these temperatures. Of course, the spherical nanoparticle would also be catalytic but with different kinetic parameters.

III. Gold Nanorods³⁶

A. Optical Properties. 1. Intense Surface Plasmon Absorption. Gold nanorods have been synthesized³⁷ electrochemically in the presence of a surfactant and cosurfactant solution mixture known to form rod-shaped micelles. A gold sheet acts as the sacrificial electrode (anode), and a platinum electrode acts as the cathode at which the gold ions are reduced. The shape distribution of the rods depends on the current and the ratio of the concentration of the surfactant to that of the cosurfactant used.

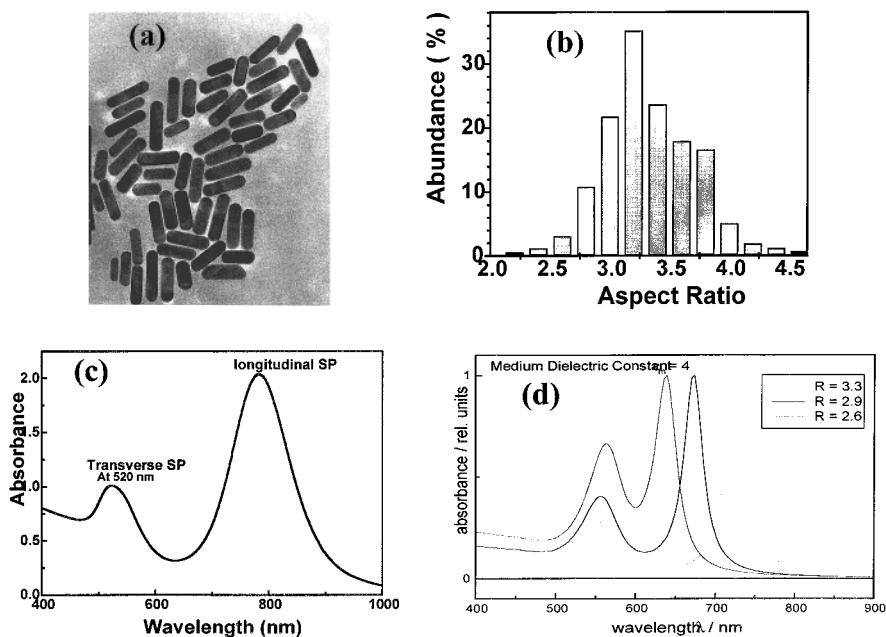


FIGURE 3. (a) TEM image of gold nanorods synthesized electrochemically in micellar solution³⁸ under the best conditions. (b) Size distribution of the nanorods. (c) Absorption spectrum of these nanorods. (d) Simulated spectra of nanorods of different aspect (length to width) ratios.

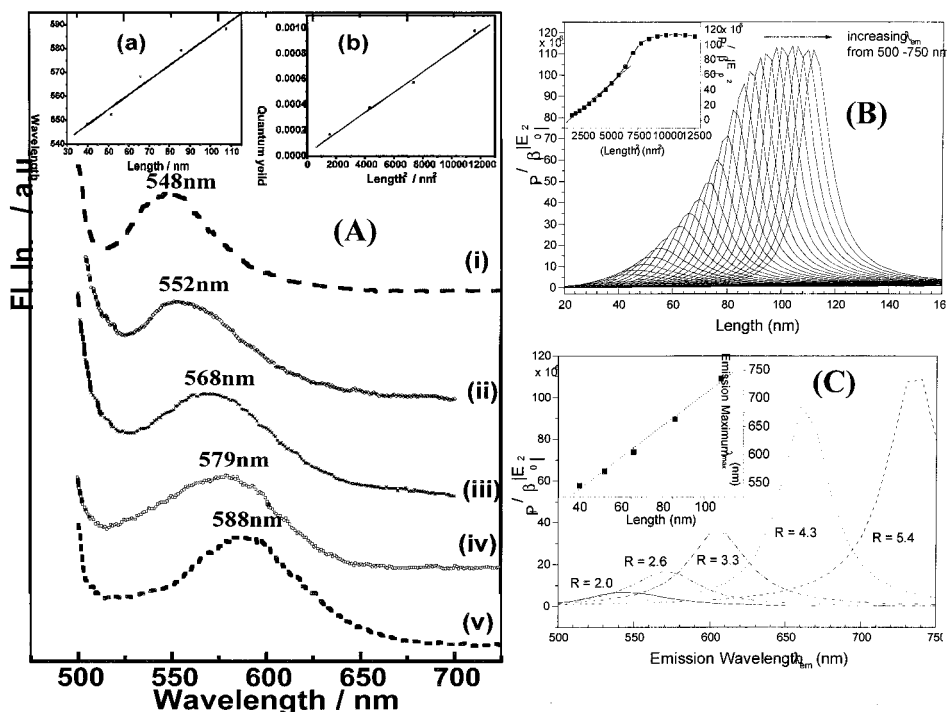


FIGURE 4. "The lightning gold nanorod".⁴² Because of the intense surface plasmon absorption of gold nanorods, the electric field of the incoming exciting light and that of the fluorescence light are greatly enhanced. This leads to an increase in the quantum yield of the fluorescence by a factor of over a million! (A-a, A-b) Dependence of both the position of the wavelength maximum and the quantum yield of the fluorescence on the rod dimension. This dependence is found⁴² to fit theoretical models,⁶³ as shown in (B) and (C).

The top part of Figure 3 shows the TEM image of the rods produced³⁸ under the best experimental conditions that gave us the best rod distribution. From the TEM images, the distribution of the aspect ratio (the ratio of the length to the width) of the rods can be determined and is shown in the top right part of Figure 3. In general, this method produces rods of widths ranging between 17 and 20 nm and lengths ranging from 40 to 200 nm.

As was discussed in the Introduction, reducing noble

metals to the nanometer length scale is associated with observing the intense surface plasmon absorption in the visible region of the spectrum. Using Maxwell's equations, Mie¹⁹ was able to derive the absorption probability due to this electronic motion in spherical particles. The shape dependence of the surface plasmon absorption was studied by Gans.³⁹ Using his equations for rod-shaped rods, the simulated absorption of the rods is shown in Figure 3d as a function of the aspect ratio.⁴⁰ The observed

absorption spectrum (Figure 3c) is much broader than the simulated one, due to the inhomogeneous broadening, which was not taken into account in the simulated spectra. Two absorption bands are shown: one is due to the coherent electronic oscillation along the short axis (the transverse absorption band), and the other (the longitudinal band) is at a longer wavelength, which is more intense and results from the coherent electronic oscillation along the long axis. The absorption maximum of the latter band is sensitive to the rod length. This absorption is over 1000 times stronger than the strongest absorption of molecular dyes! It is responsible for enhancing other linear and nonlinear processes involving the interaction of these nanoparticles with electromagnetic radiation,⁴¹ e.g., fluorescence, surface-enhanced Raman scattering, and second harmonic generation. Furthermore, the fact that the absorption intensity and wavelength maximum of these nanocrystals are sensitive to the dielectric constant of the environment (e.g., adsorbed molecules on the surface) makes them potentially useful as sensors.

2. The Lightning Gold Nanorods: Enhanced Fluorescence Yield by a Factor of Over a Million.⁴² Figure 4A shows the fluorescence emission as a function of the aspect ratio of the gold nanorods. This emission results from the interband $d \rightarrow sp$ transition, just like the very weak emission observed from gold metal surfaces, except that while the quantum yield is 10^{-11} – 10^{-10} for the metal,⁴³ we found it to be 10^{-4} – 10^{-3} for these gold nanorod solutions.⁴² This shows that in the nanorods, the fluorescence yield is enhanced by a factor of over a million!

It is observed for rods of fixed width that while the emission wavelength maximum increases with the rod length (Figure 4A-a), its quantum yield increases with the square of the rod length (Figure 4A-b). Using the model⁴⁰ developed to explain the enhancement of fluorescence from rough noble metal surfaces, we were able to simulate⁴² the fluorescence from these gold nanorods as a function of their aspect ratio (or length, since the width is the same for all the rods studied). The results of the simulation are shown in Figure 4B,C, which agree well with the observed results. This agreement supports the mechanism of the fluorescence enhancement in gold nanorods. Furthermore, it supports the previous proposal⁴¹ that roughing metal surfaces produces nanoparticles on the surface that have a strong surface plasmon absorption. This enhances the electric field of the incoming exciting light as well as that of the outgoing fluorescence (or Raman scattered) light. This is known as the field effect and leads to the enhancement of the surface fluorescence, surface Raman, and surface second harmonic generation on rough noble metal surfaces.

B. Nonradiative Photothermal Properties of Gold Nanorods. Exciting the coherent motion of the free electrons in the surface plasmon absorption by use of femtosecond laser pulses leads to a rapid dephasing of the electronic coherent oscillation due to strong electron–electron repulsion. This leads to the formation of a pulse of hot electrons of tens of thousands of degrees on the

tens of femtoseconds time scale. In the experiments described in the rest of this section, we used this short heating pulse to study the thermal properties of gold nanorods.

1. Photophysical Processes: Electron–Phonon and Phonon–Phonon Relaxation. Hot electrons relax by collision with lattice ions, resulting in heating the gold nanocrystal lattice homogeneously via electron–phonon interaction. This occurs³⁶ in ~ 1 ps. The lattice cools by giving its heat to the surrounding medium via phonon–phonon relaxation in³⁶ ~ 100 ps. These numbers have been determined from the recovery of the optical bleach of the plasmon band absorption near its maximum.^{44–55}

One of the questions that interested workers^{44–55} in this field was regarding the mechanism of the electron–phonon relaxation process. The electron mean free path in gold is near 50 nm,⁵⁶ which is longer than the size of the spherical gold nanoparticle or the transverse length of the nanorod. This raises the question about the contribution of surface scattering processes to the electron–phonon relaxation process. This would predict that the rate of this process should depend on the size and shape of the nanoparticle.

We have determined^{36,44–47} the electron–phonon relaxation times for different sizes of spherical nanoparticles as well as for the relaxation of the transverse and longitudinal excitation of gold nanorods. Correcting for laser power effects, this time is found to be ~ 1 ps for gold nanospheres of different sizes and for the transverse as well as for longitudinal relaxation of the gold nanorods. Using the theory originally developed for the contribution of surface scattering,⁵⁷ Hartland et al.⁵⁸ were able to show that the contribution of surface scattering in gold nanodots is $< 10\%$. This is due to the fact that surface vibronic interaction is proportional⁵⁷ to the ratio of the number of valence electrons per atom (the one 6s electron in Au) to the atomic mass (200). This being very small ($1/200$) for gold explains the lack of size or shape dependence of the electron–phonon process. For a lighter atom with more valence electrons, e.g., Al, strong surface scattering of its nanoparticles ought to be observed, leading to shape-dependent electron–phonon relaxation processes. This has already been reported for tin and Ga observed by femtosecond transient reflectivity measurements.^{59,60}

2. Controlled Laser Photothermal Nonradiative Shape Transformation Processes. (i) How Long⁶¹ and How Much Energy⁶² Does It Take To Transform a Gold Nanorod into a Nanosphere? A solution of the nanorods was exposed to a number of pulses having 100-fs pulse width of the appropriate energy while being continuously stirred, and the continuous-wave absorption spectrum was continuously monitored. When the longitudinal band disappeared, a drop of the solution was dried on a TEM slide, and the TEM images were determined. If the energy used was at the threshold, it was found⁶³ that the image contained only spheres of number of atoms comparable to those of the original rods (see Figure 5b). This suggests that exposure to the femtosecond pulses used leads to complete transformation into spheres. With the knowl-

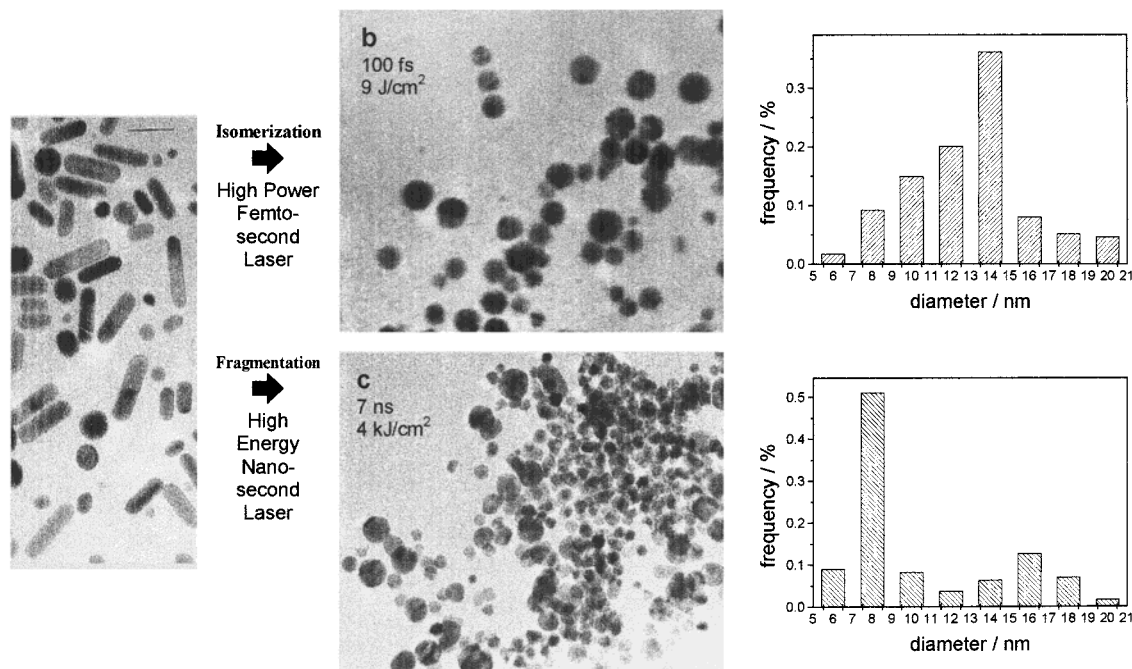


FIGURE 5. Dependence of the photothermal laser transformation of gold nanorods in micellar solution on the laser pulse energy and pulse width.⁶⁶ (b) Irradiation with femtosecond pulses of controlled energy give rise to spheres with number of atoms comparable to that of the parent nanorods (photothermal isomerization), while (c) high-energy nanosecond pulses give rise to photothermal fragmentation into small spheres.

edge of the amount of energy delivered to the rods in solution, their absorption coefficient, and their concentration, the amount of energy needed to transform a gold nanorod into a sphere was determined⁶² to be ≥ 60 fJ.

Another question arises as to how long it takes to transform the nanorod into a sphere in solution. By heating the rod with 100-fs laser pulses of the threshold energy and monitoring the decay of the longitudinal absorption band, it was possible⁶¹ to determine the time of the change of the shape of the gold nanorod. This is found to be 35 ± 5 ps. The question thus arises as to whether this time corresponds to the complete melting of the rod or to a partial change in the configuration, leading to the decrease in the absorption at the monitoring wavelength. A TEM study of the resulting transformed nanoparticles at these pulse energies leads to the conclusion that 35 ps is, indeed, the time of complete rod-to-sphere transformation.

From the previous section, we have learned that hot electrons resulting from laser photoexcitation heat the lattice in ~ 1 ps. To change the structure of the ions in the lattice, we need to accumulate sufficient heat in the lattice at a rate faster than the rate of cooling it. The time constant for the latter process is found to be near 100 ps. Thus, the 35-ps decay time of the longitudinal absorption band is between the time required to heat the lattice with the photothermally formed hot electrons (~ 1 ps) and that required for cooling it by phonon–phonon relaxation processes to the solvent (~ 100 ps). This suggests that melting could, indeed, occur in 35 ps.

One more requirement needs to be satisfied. The melting time cannot be faster than the travel time of a sound wave in the nanorod. This is calculated to be 15

ps. Thus, the observed time of decay of the longitudinal absorption band in our experiment strongly suggests that the melting of the gold nanorod occurs on the 35-ps time scale.

(ii) Laser Photofragmentation of Gold Nanorods.⁶³ If the energy of the femtosecond pulse is increased above the threshold of transforming the rods into spheres, fragmentation into smaller spheres is observed. Obviously, if the rate of photothermal heating increases, the internal energy of the lattice increases and high-energy channels above that of melting open up. These high-energy channels are the different fragmentation channels. If nanosecond laser pulses are used, photofragmentation is also observed (Figure 5c). The results of photothermal transformation of the rod with nanosecond laser excitation are interesting. It seems that having a longer pulse assists in opening up the fragmentation channels, suggesting that after heating of the lattice, more photon absorption takes place during the longer nanosecond pulse, which leads to an increase in the lattice internal energy that opens up the fragmentation channels.⁶³

To test the above proposal, we have used femtosecond laser pulses having the threshold energy required to melt (but not to fragment) the nanorods in solution to spheres. The pulse train was then split into two, and the sample solution was irradiated with the two pulses overlapping in space but separated from one another in time by different delays. At each delay, and after irradiation with the two pulses repeatedly for a fixed length of time while the sample was being continuously stirred, a drop of the solution was spotted and dried, and the TEM images were recorded. From the TEM pictures, the average size of the spheres resulting from the irradiation at each delay time

was determined and plotted against the delay time between the pulses. It was observed that when the delay time was in the >3 –100-ps range, fragmentation was observed. At delay times shorter than a few picoseconds or longer than 100 ps, only melting without fragmentation was observed. The results were similar to those observed when only one pulse was used. This suggests that if the second pulse is absorbed while the lattice is hot (i.e., during a period longer than electron–phonon relaxation time, ~ 1 ps, but shorter than phonon–phonon relaxation time, <100 ps), more absorption can take place, which leads to fragmentation. If the lattice heated by absorbing the first pulse is allowed to cool by phonon–phonon relaxation processes (>80 ps), either photons from the second pulse are not absorbed or, if they are, they only melt the spheres again. This does not lead to fragmentation. If the second pulse arrives before the excited electrons from absorbing the first pulse (i.e., <1 ps) heat the lattice, it is absorbed by the cool lattice and thus does not seem to cause fragmentation.

(iii) Thermal and Laser Photothermal Shaping of Gold Nanorods in Micellar Solution. (a) Thermal Reshaping.³⁸ We found that slow heating of a solution of gold nanorods capped with micelles in an oil bath dissolves the long micelles (leading to the precipitation of these gold nanorods out of solution) at temperatures lower than those required to dissolve the shorter micelles. This leads to a decrease in the average length of the rods remaining in solution and a blue shift of the longitudinal absorption maximum. Thus, by using optical spectroscopy, the thermal stability (or the solubility) of the micelles can be studied as a function of their length. Equally important, it is a simple method to reshape the size distribution of gold nanorods.

(b) Laser Photothermal Reshaping.⁶⁴ Since the absorption spectrum of a gold nanorod solution is broad due to its wide size distribution, it is possible to heat and change the shape of, e.g., the longest rods (leaving the rest unexcited) by simply adjusting the pump laser wavelength to the longest absorption wavelength edge of the longitudinal band. By using physical methods, the changed shape can be separated from the solution. This gives rise to a narrower and shorter size distribution. This is another method by which the size distribution of gold nanorods can be narrowed and reshaped.

In summary, gold nanorods are shown to have interesting properties. They have 10 million times higher fluorescence yield than gold metals. This is shown to result from the field effect due to coupling of the electromagnetic radiation to the strongly absorbing surface plasmon oscillations present in these nanorods. The electron–phonon relaxation time in these nanorods is found to be ~ 1 ps, independent of shape or size. This indicates the lack of contribution of surface scattering to the relaxation process. The lattice cools in ~ 100 ps, and the nanorods are transformed into spheres in 35 ps by absorbing >60 fJ per rod. If the energy is increased or if lasers of nanosecond pulse width are used, fragmentation to smaller spheres takes place. It is found that, by thermal

heating to a specific temperature, reshaping the rod distribution to smaller rods can be obtained. This is due to the lower solubility of the large capping micelles at higher temperatures. Laser photothermal reshaping of the rods can also be accomplished by burning optical holes in the long-wavelength longitudinal absorption band by lasers of energies sufficient to change the shape of the excited rods.

I thank the members of our group at the Laser Dynamics Laboratory who have carried out the work described here: T. Ahmadi, Dr. C. Burda, Dr. K. Ismail, Y. Li, S. Link, M. B. Mohamed, B. Nikoobakht, J. Petroski, and V. Volkov. The collaboration with Professor Z. L. Wang of the material science department at Georgia Tech has been very fruitful. We thank him for the use of his TEM facility as well. I thank the National Science Foundation (Grant No. CHE-9727633) for the support of this work.

References

- (1) Steigerwald, M. L.; Brus, L. E. Semiconductor Crystallites: A Class of Large Molecules. *Acc. Chem. Res.* **1990**, *23*, 183.
- (2) Wang, Y.; Herron, N. Nanometer-Sized Semiconductor Clusters: Materials Synthesis, Quantum Size Effects, and Photophysical Properties. *J. Phys. Chem.* **1991**, *95*, 525 (feature article).
- (3) Wang, Y. In *Advances in Photochemistry*; Neckers, D. C., Ed.; John Wiley & Sons: New York, 1995; Vol. 19, p 179.
- (4) Haase, M.; Weller, H.; Henglein, A. Photochemistry of Colloidal Semiconductors. 26. Photoelectron Emission from Particles and Related Chemical Effect. *J. Phys. Chem.* **1988**, *92*, 4706.
- (5) Chestnoy, N.; Harris, T. D.; Hull, R.; Brus, L. E. Luminescence and Photophysics of CdS Semiconductor Clusters: The Nature of Emitting Electronic State. *J. Phys. Chem.* **1986**, *90*, 3393.
- (6) Brus, L. E. Electron–electron and Electron–hole Interactions in Small Semiconductor Crystallites: the Size Dependence of the Lowest Excited Electronic State. *J. Chem. Phys.* **1984**, *80*, 4403–4409.
- (7) Brus, L. Zero-dimensional ‘Excitons’ in Semiconductor Clusters. *IEEE J. Quantum Electron.* **1986**, *QE-22*, 1909–1914.
- (8) Alivisatos, A. P.; Harris, A. L.; Levinos, N. J.; Steigerwald, M. L.; Brus, L. E. Electronic States of Semiconductor Clusters: Homogeneous and Inhomogeneous Broadening of the Optical Spectrum. *J. Chem. Phys.* **1988**, *89*, 4001–4011.
- (9) Kamat, P. V. Interfacial Charge-Transfer Processes in Colloidal Semiconductor Systems. *Prog. React. Kinet.* **1994**, *19*, 277–316.
- (10) Heath, J. R. The Chemistry of Size and Order on the Nanometer Scale. *Science* **1995**, *270*, 1315–1316.
- (11) Murray, C. B.; Kagan, C. R.; Bawendi, M. G. Self-Organization of CdSe Nanocrystallites Into Three-Dimensional Quantum Dot Superlattices. *Science* **1995**, *270*, 1335–1338.
- (12) Alivisatos, A. P. Perspective on the Physical Chemistry of Semiconductor Nanocrystals. *J. Phys. Chem.* **1996**, *100*, 13226.
- (13) Zhang, J. Z. Ultrafast Studies of Electron Dynamics in Semiconductor and Metal Colloidal Nanoparticles: Effects of Size and Surface. *Acc. Chem. Res.* **1997**, *30*, 423–429.
- (14) Kreibitz, U.; Vollmer, M. *Optical Properties of Metal Clusters*; Springer: Berlin, 1995.
- (15) Papavassiliou, G. C. Optical Properties of Small Inorganic and Organic Metal Particles. *Prog. Solid State Chem.* **1979**, *12*, 185.
- (16) Kerker, M. *The Scattering of Light and Other Electromagnetic Radiation*; Academic Press: New York, 1969.
- (17) Bohren, C. F.; Huffman, D. R. *Absorption and Scattering of Light by Small Particles*; Wiley: New York, 1983.
- (18) Kerker, M. The Optics of Colloidal Silver: Something Old and Something New. *J. Colloid Interface Sci.* **1985**, *105*, 297.
- (19) Mie, G. Optical Properties of Colloidal Gold Solutions. *Ann. Phys.* **1908**, *25*, 329.
- (20) Creighton, J. A.; Eadon, D. G. Ultraviolet–Visible Absorption Spectra of the Colloidal Metallic Elements. *J. Chem. Soc., Faraday Trans.* **1991**, *87*, 3881.
- (21) Mulvaney, P. Surface Plasmon Spectroscopy of Nanosized Metal Particles. *Langmuir* **1996**, *12*, 788.
- (22) Hirai, H.; Wakabayashi, H.; Komiyama, M. Polymer-Protected Copper Colloids As Catalysts For Selective Hydration Of Acrylonitrile. *Chem. Lett.* **1983**, 1047.
- (23) Brugger, P.-A.; Cuendet, P.; Gratzel, M. Ultrafine and Specific Catalysts Affording Efficient Hydrogen Evolution from Water under Visible Light Illumination. *J. Am. Chem. Soc.* **1981**, *103*, 2923.

- (24) Thomas, J. M. Colloidal Metals: Past, Present and Future. *Pure Appl. Chem.* **1988**, *60*, 1517.
- (25) Charles, S. C.; Popplewell, J. In *Ferromagnetic Materials*; Wohlfarth, E. P., Ed.; North-Holland: Amsterdam, 1980; Vol. 2.
- (26) Schön, G.; Simon, U. A Fascinating New Field in Colloidal Science: Small Ligand-Stabilized Metal Clusters and Their Possible Application in Microelectronics *Colloid Polym. Sci.* **1995**, *273*, 202.
- (27) Ahmadi, T.; Wang, Z. L.; Green, T. C.; Henglein, A.; El-Sayed, M. A. Shape Controlled Synthesis of Colloidal Platinum Nanoparticles. *Science* **1996**, *272*, 1924.
- (28) Watzky, M. A.; Finke, R. G. Transition Metal Nanocluster Formation Kinetic and Mechanistic Studies. A New Mechanism When Hydrogen Is the Reductant: Slow, Continuous Nucleation and Fast Autocatalytic Surface Growth. *J. Am. Chem. Soc.* **1997**, *119*, 10382.
- (29) Petroski, J. M.; Wang, Z. L.; Green, T. C.; El-Sayed, M. A. Kinetically Controlled Growth and Shape Formation Mechanism of Platinum Nanoparticles. *J. Phys. Chem. B* **1998**, *102*, 3316.
- (30) Li, Y.; Petroski, J. M.; El-Sayed, M. A. The Activation Energy of the Reaction between Hexacyanoferrate(III) and Thiosulphate Ions Catalyzed by Platinum Nanoparticles. *J. Phys. Chem.* **2000**, *104*, 10956.
- (31) Ahmadi, T. Colloidal Metallic and Gaseous Ionic Nanoparticles: Structure, Dynamics, and Catalysis. Ph.D. Thesis, Georgia Institute of Technology, 1996.
- (32) (a) Miyaura, N.; Yanagi, T.; Suzuki, A. The Palladium-Catalyzed Cross-Coupling Reaction of Phenylboronic Acid with Haloarenes in the Presence of Bases. *Synth. Commun.* **1981**, *11*, 513. (b) Suzuki, A. In *Metal-catalyzed Cross-Coupling Reactions*; Diederich, F., Stang, P. J., Eds.; VCH: Weinheim, 1998; pp 49–97.
- (33) Reetz, M. T.; Breinbauer, R.; Wanninger, K. Suzuki and Heck Reactions Catalyzed by Preformed Palladium Clusters and Palladium/Nickel Bimetallic Clusters. *Tetrahedron Lett.* **1996**, *37*, 4499–4502.
- (34) Li, Y.; Hong, X. M.; Collard, D. M.; El-Sayed, M. A. Suzuki Cross-Coupling Reactions Catalyzed by Palladium Nanoparticles. *Org. Lett.* **2000**, *15*, 2385–2388.
- (35) Wang, Z. L.; Petroski, J. M.; Green, T. C.; El-Sayed, M. A. Shape Transformation and Surface Melting of Cubic and Tetrahedral Platinum Nanocrystals. *J. Phys. Chem. B* **1998**, *102*, 6145.
- (36) For a recent review, see: Link, S.; El-Sayed, M. A. Spectral Properties and Relaxation Dynamics of Surface Plasmon Electronic Oscillations in Gold and Silver Nanodots and Nanorods. *J. Phys. Chem. B* **1999**, *103*, 8410–8426 (Feature Article).
- (37) Yu, Y.-Y.; Chang, S.-S.; Lee, C. -L.; Wang, C. R. C. Gold Nanorods: Electrochemical Synthesis and Optical Properties. *J. Phys. Chem. B* **1997**, *101*, 6661.
- (38) Mohamed, M. B.; Ismail, K. Z.; Link, S.; El-Sayed, M. A. Thermal Reshaping of Gold Nanorods in Micelles. *J. Phys. Chem. B* **1998**, *102*, 9370.
- (39) Gans, R. Form of Ultramicroscopic Particles of Silver. *Ann. Phys.* **1915**, *47*, 270.
- (40) Link, S.; Mohamed, M. B.; El-Sayed, M. A. Simulation of the Optical Absorption Spectra of Gold Nanorods as a Function of Their Aspect Ratio and the Effect of the Medium Dielectric Constant *J. Phys. Chem. B* **1999**, *103*, 3073.
- (41) Boyd, G. T.; Yu, Z. H.; Shen, Y. R. Photoinduced Luminescence from the Noble Metals and its Enhancement on Roughened Surfaces. *Phys. Rev. B* **1986**, *33*, 7923.
- (42) Mohamed, M. B.; Volkov, V.; Link, S.; El-Sayed, M. A. The “Lightning” Gold Nanorods: Fluorescence Enhancement of over a Million Compared to the Gold Metal. *Chem. Phys. Lett.* **2000**, *317*, 517.
- (43) Mooradian, A. Photoluminescence of Metals. *Phys. Rev. Lett.* **1969**, 185.
- (44) Ahmadi, T. S.; Logunov, S. L.; El-Sayed, M. A. Picosecond Dynamics of Colloidal Gold Nanoparticles. *J. Phys. Chem.* **1996**, *100*, 8053–8056.
- (45) Ahmadi, T. S.; Logunov, S. L.; El-Sayed, M. A.; Khoury, J. T.; Whetten, R. L. Electron Dynamics of Passivated Gold Nanocrystals Probed by Subpicosecond Transient Absorption. *J. Phys. Chem. B* **1997**, *101*, 3713–3719.
- (46) Link, S.; Burda, C.; Wang, Z. L.; El-Sayed, M. A. Electron Dynamics In Gold And Gold–Silver Alloy Nanoparticles: The Influence Of A Nonequilibrium Electron Distribution And The Size Dependence Of The Electron–Phonon Relaxation. *J. Chem. Phys.* **1999**, *111*, 1255.
- (47) Link, S.; Burda, C.; Mohamed, M. B.; Nikoobakht, B.; El-Sayed, M. A. Femtosecond Transient-Absorption of Colloidal Gold Nanorods: Shape Independence of the Electron–Phonon Relaxation Time. *Phys. Rev. B* **2000**, *61*, 6086–6090.
- (48) Perner, M.; Bost, P.; von Plessen, G.; Feldmann, J.; Becker, U.; Mennig, M.; Schmitt, M.; Schmidt, H. Optically Induced Damping of The Surface Plasmon Resonance in Gold Colloids. *Phys. Rev. Lett.* **1997**, *78*, 2192.
- (49) Del Fatti, N.; Vallee, F.; Flytzanis, C.; Hamanaka, Y.; Nakamura, A. Electron dynamics and surface plasmon resonance nonlinearities in metal nanoparticles. *Chem. Phys.* **2000**, *251*, 215.
- (50) Hodak, J. K.; Martini, I.; Hartland, G. V. Spectroscopy and Dynamics of Nanometers-Sized Noble Metal Particles. *J. Phys. Chem. B* **1998**, *102*, 6958.
- (51) Bigot, J.-Y.; Halte, V.; Merle, J.-C.; Daunois, A. Electron dynamics in metallic nanoparticles. *Chem. Phys.* **2000**, *251*, 181.
- (52) Smith, B. A.; Zhang, J. Z.; Giebel, U.; Schmid, G. Direct Probe of Size-Dependent Electronic Relaxation in Single-Sized Au and Nearly Monodisperse Pt Colloidal Nanoparticles. *Chem. Phys. Lett.* **1997**, *270*, 139.
- (53) Inouye, H.; Tanaka, K.; Tanahashi, I.; Hirao, K. Ultrafast Dynamics of Nonequilibrium Electrons in a Gold Nanoparticles System. *Phys. Rev. B* **1998**, *57*, 11334.
- (54) Averitt, R. D.; Westcott, S. L.; Halas, N. J. Ultrafast Dynamics in Gold Nanoshells *Phys. Rev. B* **1998**, *58*, 10203.
- (55) Hodak, J. K.; Martini, I.; Hartland, G. V. Ultrafast Study of Electron–Phonon Coupling in Colloidal Gold Particles. *Chem. Phys. Lett.* **1998**, *284*, 135.
- (56) Kittel, C. *Introduction to Solid State Physics*; Wiley: New York, 1996.
- (57) (a) Belotskii, E. D.; Tomchuk, P. M. Surface Electron–Phonon Energy Exchange in Small Metallic Particles. *Int. J. Electron.* **1992**, *73*, 955. (b) Belotskii, E. D.; Tomchuk, P. M. Electron–Phonon Interaction and Hot Electron in Small Metal Islands. *Surf. Sci.* **1990**, *239*, 143.
- (58) Hodak, J. H.; Henglein, A.; Hartland, G. V. Electron–phonon coupling dynamics in very small (between 2 and 8 nm diameter) Au nanoparticles. *J. Chem. Phys.* **2000**, *112*, 5942.
- (59) Stella, A.; Nisoli, M.; De Silvestri, S.; Svelto, O.; Lanzani, G.; Cheyssac, P.; Kofman, R. Size effect in the Ultrafast Electronic Dynamics of Metallic Tin Nanoparticles. *Phys. Rev. B* **1996**, *53*, 15497.
- (60) Nisoli, M.; Stagira, S.; De Silvestri, D. Ultrafast Electronic Dynamics in Solid and Liquid Gallium Nanoparticles. *Phys. Rev. Lett.* **1997**, *78*, 3575.
- (61) Link, S.; Burda, C.; Nikoobakht, B.; El-Sayed, M. A. How long does it take to melt a gold nanorod? A femtosecond pump–probe absorption spectroscopic study. *Chem. Phys. Lett.* **1999**, *315*, 12.
- (62) Link, S.; El-Sayed, M. A. *J. Chem. Phys.* submitted.
- (63) Link, S.; Burda, C.; Mohamed, M. B.; Nikoobakht, B.; El-Sayed, M. A. Laser Photothermal Melting and Fragmentation of Gold Nanorods: Energy and Laser Pulse-Width Dependence. *J. Phys. Chem. A* **1999**, *103*, 1165.
- (64) Link, S.; Burda, C.; Nikoobakht, B.; El-Sayed, M. A. Laser-Induced Shape Changes of Colloidal Gold Nanorods Using Femtosecond and Nanosecond Laser Pulses. *J. Phys. Chem. B* **2000**, *104*, 6152–6163.

AR960016N